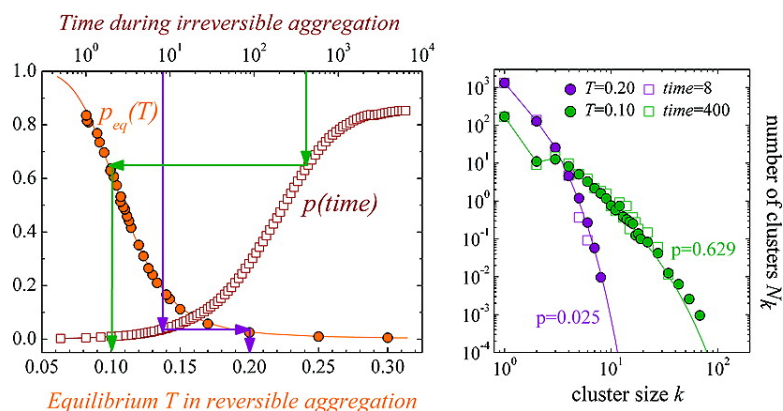


Connecting Irreversible to Reversible Aggregation: Time and Temperature

S. Corezzi, C. De Michele, E. Zaccarelli, P. Tartaglia, and F. Sciortino

J. Phys. Chem. B, **2009**, 113 (5), 1233-1236 • DOI: 10.1021/jp809031d • Publication Date (Web): 13 January 2009

Downloaded from <http://pubs.acs.org> on February 5, 2009



More About This Article

Additional resources and features associated with this article are available within the HTML version:

- Supporting Information
- Access to high resolution figures
- Links to articles and content related to this article
- Copyright permission to reproduce figures and/or text from this article

[View the Full Text HTML](#)



Connecting Irreversible to Reversible Aggregation: Time and Temperature

S. Corezzi,^{*,†} C. De Michele,^{‡,§} E. Zaccarelli,^{‡,§} P. Tartaglia,^{§,||} and F. Sciortino^{‡,§}

CNR-INFM Polylab, CNR-INFM Polylab, Largo Pontecorvo 3, I-56127 Pisa, Italy, and CNR-INFM SOFT, Dipartimento di Fisica, and CNR-INFM SMC, Università di Roma “La Sapienza”, Piazzale A. Moro 2, I-00185 Roma, Italy

Received: October 12, 2008

We report molecular dynamics simulations of a gel-forming mixture of ellipsoidal patchy particles with different functionality. We show that in this model, which disfavors the formation of bond-loops, elapsed time during irreversible aggregation—leading to the formation of an extended network—can be formally correlated with equilibrium temperature in reversible aggregation. We also show that it is possible to develop a parameter-free description of the self-assembly kinetics, bringing reversible and irreversible aggregation of loopless branched systems to the same level of understanding as equilibrium polymerization.

Several natural and synthetic materials, as well as biological structures, result from the self-assembly of elementary units into branched aggregates and networks.^{1–5} This self-assembly process is receiving considerable attention in two fast-growing fields: supramolecular chemistry^{1–3} and collective behavior of patchy and functionalized particles,^{6–8} among the most promising building blocks of new materials.^{9,10} The process of formation of an extended three-dimensional network of bonds connecting independent molecules, proteins or colloidal particles, is named gelation and the resulting material a gel.^{11–13} The ratio between the bond energy u_0 and the thermal energy $k_B T$ (where k_B is the Boltzmann constant and T is the temperature) can be used to classify aggregation into two broad categories: For strong attraction strength (*chemical case*),^{11,14–16} bond formation is irreversible and the number of bonds continuously grows with time. In the case of weak attraction strength (*physical case*),¹⁷ bonds break and reform while the number of bonds progressively reaches its equilibrium value. In the latter case, the final structure of the system can in principle be predicted with equilibrium statistical mechanics methods.

The value of the ratio $u_0/k_B T$ separates the two classes. Conceptually, any model of physical aggregation may be turned into a chemical model by studying its properties following a quench to $k_B T \ll u_0$. Similarly, applying temperatures comparable to the bond energy turns an irreversible aggregation model into a physical one. The idea of a close connection between irreversible and reversible aggregation is already contained in the early mean-field theoretical work of Stockmayer,¹⁴ considering the Smoluchowski's kinetic equations solved in the limit of absence of closed bonding loops. In Stockmayer's calculations, at any time t during chemical aggregation, the distribution of clusters of finite size k ($N_k(t)$) is identical to that found following equilibrium statistical mechanics prescriptions, i.e., by maximizing the entropy with the constraint of a fixed number

of bonds. The N_k are commonly referred to as Flory–Stockmayer (FS) distributions. Later on, Van Dongen and Ernst¹⁸ confirmed that the FS distributions are also solutions of the Smoluchowski's equations when bond-breaking processes are accounted for. According to these theoretical works—based on kinetic equations derived in the limit of reaction-controlled rates (as opposed to diffusion-controlled)¹⁹—a system forming progressively larger and larger loopless branched aggregates evolves in time via a sequence of states which are identical to the states explored in equilibrium at appropriate values of T . The equality in the fraction of formed bonds p (the extent of reaction in chemical language) provides the connection between t during *reversible* or *irreversible* aggregation and T in *equilibrium*. Van Dongen and Ernst¹⁸ also provide an analytic expression for the t -dependence of p following a sudden change in the external control parameters, offering the first soluble example of reversible self-assembly of loopless branched structures. Interestingly, for functionality two (chain assembly) the solution coincides with the mean-field analytic expressions later on derived for equilibrium polymerization kinetics.²⁰ Despite their relevance, to our knowledge, the Van Dongen and Ernst predictions have never been tested experimentally or numerically to assess their limit of validity.

In this letter—stimulated by the renewed interest in reversible and irreversible self-assembly of nano- and microparticles interacting via specific directional bonds^{1,2,6–8}—we provide a stringent test of the suggested connections between chemical and physical aggregation, and establish the limits of analytic description of the kinetics of formation of branched structures. We do so by extending a model for chemical gels, recently introduced,²¹ to the corresponding physical case by turning the attraction strength between bonding sites finite. The model, originally inspired by epoxy–amine step-polymerization,²² represents two types of mutually reactive molecules A and B as hard homogeneous ellipsoids of revolution whose surface is decorated in a predefined geometry by f_A and f_B identical reactive sites. The study of the chemical version of this model²¹ showed that formation of closed bonding loops in finite size clusters is disfavored, possibly due to the nonspherical particle shape and

[†] Università di Pisa.[‡] CNR-INFM SOFT.[§] Dipartimento di Fisica, Università di Roma “La Sapienza”.^{||} CNR-INFM SMC, Università di Roma “La Sapienza”.

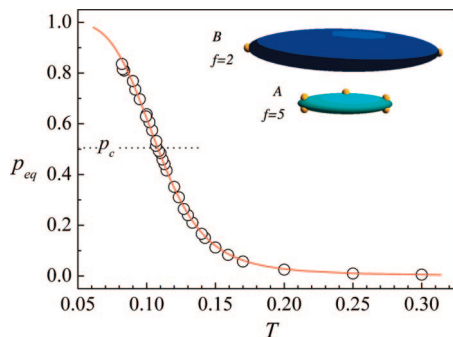


Figure 1. Temperature dependence of the fraction of bonds at equilibrium, p_{eq} : (symbols) simulation results. The solid line represents $p_{eq}(T)$ from eq 1. A one-parameter best-fit gives $\Delta S/k_B = 8.52$. The percolation threshold $p_c = 0.5$ is indicated by a horizontal line. The inset shows a graphic description of the A and B particles. The centers of the small spheres locate the bonding sites on the surface of the hard-core ellipsoid.

the location of the reactive sites. Therefore, it offers to us the possibility to carefully check the Stockmayer¹⁴ and Van Dongen and Ernst¹⁸ predictions. We can assess how closely—in the absence of loop formation—the chemical gelation process in a system of functionalized or patchy units, as well as the reversible evolution from a monomeric to an equilibrium bonded state, can be envisaged as a progressive sequence of equilibrium states, closely connecting t with T .

We study via event-driven molecular dynamics simulations a binary mixture composed of $N_A = 480$ pentafunctional ($f_A = 5$) ellipsoids of type A and $N_B = 1200$ bifunctional ($f_B = 2$) ellipsoids of type B, so that the number $N_A f_A$ of A-type reactive sites equals the number $N_B f_B$ of B-type reactive sites. A particles have mass m , revolution axis $a = 10\sigma$, and the other two axes $b = c = 2\sigma$; B particles have mass $3.4m$ and axes $a = 20\sigma$ and $b = c = 4\sigma$. Size- and mass-ratios are chosen to mimic the values of an epoxy–amine system.²² The interaction potential is the hard ellipsoid potential V_{HE} supplemented by site–site square-well attractive interactions V_{SW} (of strength u_0 , and width $\delta = 0.2\sigma$) between pairs of particles of different type. Our unit mass is m , and the unit of energy is u_0 . T is measured in units of the potential depth (i.e., $k_B = 1$), time t in units of $\sigma(mlu_0)^{1/2}$. The packing fraction is fixed at $\phi = 0.3$ and T is varied from $T = 0.3$ to 0.065 . Event-driven (newtonian) molecular dynamics simulations (in the NVT ensemble) are performed using a specifically designed code.²³ Two sites, on particles of different type, form a bond if their distance is closer than δ . Clusters are defined as groups of bonded particles. The particle shape and the location of the attractive sites (see inset of Figure 1) is such that each site is engaged at most in one bond, ensuring an unambiguous definition of the extent of reaction p by the ratio between the number of bonds in the system and the maximum number of possible bonds (i.e., $N_A f_A$). Unless otherwise stated, we study the trajectory of the system in configuration space, starting from an initial configuration with no bonds between particles, at fixed T . During the simulation, bonds form and break continuously with time while the system evolves toward the equilibrium state, characterized by an equilibrium value $p_{eq}(T)$ of the extent of reaction. To improve the statistics, we average over 11 different realizations for each studied T . Equilibrium results are obtained from the final part of the trajectories, after the equilibration transient is over.

Figure 1 shows $p_{eq}(T)$ for all T values where equilibration was achieved within the allocated computational time (six months at low T). Within the range $0.2 > k_B T/u_0 > 0.08$, the system crosses from a monomeric state to a significantly bonded

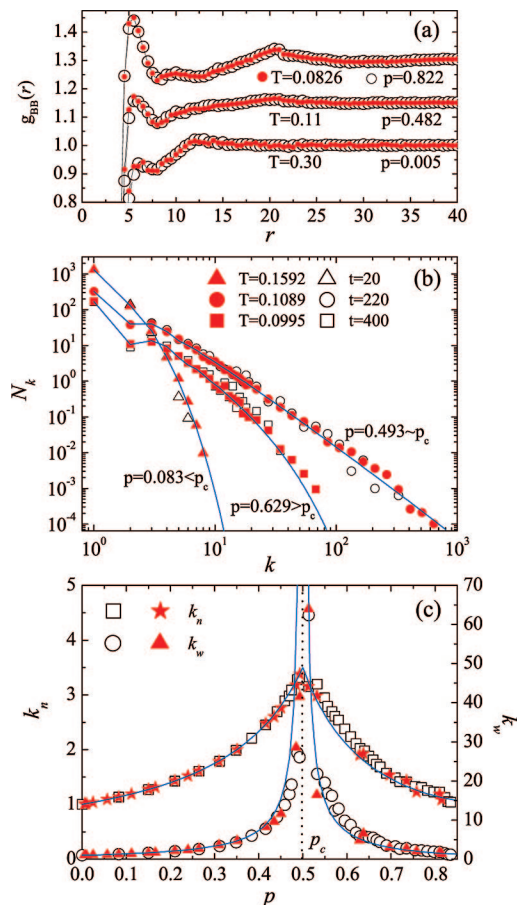


Figure 2. (a) Partial radial distribution function for B particles, $g_{BB}(r)$. (b) Cluster size distribution N_k . (c) Number- and weight-average size of the finite clusters (k_n and k_w). In all panels, equilibrium results (closed symbols) are compared with results at different times t during irreversible aggregation (open symbols, from ref 21) such that $p(t) = p_{eq}(T)$. In panel a, curves at $T = 0.11$ and 0.0826 are shifted by $+0.15$ and $+0.30$, respectively. In b and c, solid lines indicate FS predictions.

state, with more than 80% of the bonds formed. The sharp sigmoidal shape can be perfectly represented by the independent-bond mass-action law²⁴

$$\frac{P_{eq}}{(1 - P_{eq})^2} = e^{\beta(u_0 - T\Delta S)} \quad (1)$$

where u_0 and ΔS describe, respectively, the energy and the entropy change associated to the formation of a single bond.

Figure 2a and b shows the equilibrium structure of the system and the cluster size distribution N_k at three different values of T , corresponding to p_{eq} values below, at, and above percolation (numerically located at $p_c = 0.505 \pm 0.007$).²¹ To describe the structure of the system, we report the center-to-center pair distribution function $g_{BB}(r)$ for the B particles. To quantify the T dependence of N_k we also report the number- (k_n) and weight-average size (k_w) of the finite clusters (Figure 2c). Data shown in Figure 2b and c are very well described—without any fitting parameter—both below and above percolation by the FS predictions^{15,21} specialized to the $f_A = 5 - f_B = 2$ case, confirming that bonding loops in finite size clusters can be neglected. Therefore, the model allows us to check, without fitting parameters, if the evolution of the system during equilibration and irreversible aggregation does follow a sequence of equi-

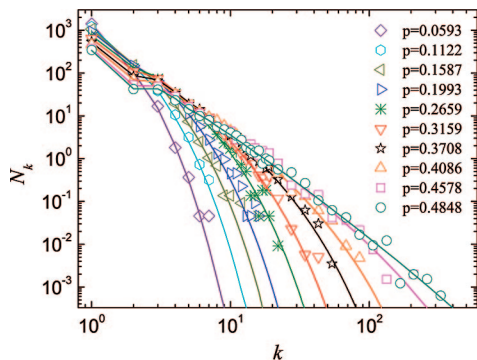


Figure 3. Distribution of finite size clusters N_k for different times (and fraction of bonds p) during reversible aggregation following a T -jump to $T = 0.11$. At each time during the equilibration process, the cluster size distribution is identical to the FS distribution at the same fraction of bonds (solid lines).

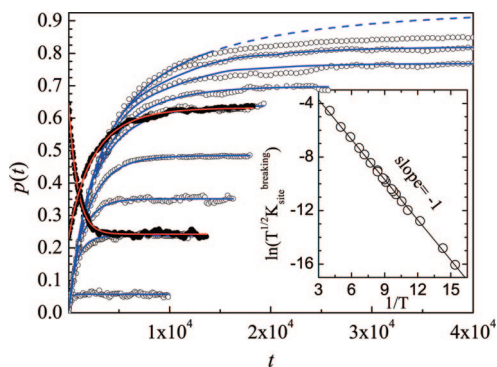


Figure 4. Time dependence of the fraction of bonds $p(t)$ during reversible aggregation at different temperatures ($T = 0.17, 0.13, 0.12, 0.11, 0.10, 0.095, 0.09, 0.082$, and 0.07 from the lower to the higher equilibrium value $p(\infty) = p_{\text{eq}}$, starting from an unbonded configuration ($p(0) = 0$; open symbols) or from a generic equilibrated configuration ($p(0) \neq 0$; closed symbols). Lines are solutions of the Smoluchowski's equation for reversible aggregation (eq 2), with p_{eq} from eq 1 and $K_{\text{site}}^{\text{breaking}}$ as the only fit parameter. The inset shows the T dependence of $K_{\text{site}}^{\text{breaking}}$.

librium steps, and in particular, how t in chemical gelation can be associated to a corresponding equilibrium T . To this aim, we compare in Figure 2a–c the equilibrium quantities with the corresponding quantities evaluated at selected elapsed times t during the irreversible bonding process. The specific t value is chosen in such a way that $p(t) = p_{\text{eq}}(T)$. For all these quantities, at each t , data are identical to those obtained in equilibrium at the same extent of reaction, demonstrating that the evolution of the system structure and connectivity during irreversible aggregation does follow a sequence of equilibrium states.

Also the equilibration process at finite T , i.e., when bond-breaking processes are included, proceeds along a sequence of equilibrium states described by the FS theory. Indeed, Figure 3 shows $N_k(t)$ for several successive times following a quench, in conditions of reversible aggregation, from a high- T un-assembled state to a low- T assembled one. Data are compared—without fit parameters—with the corresponding equilibrium quantities, accurately modeled by the FS distributions. Similar agreement is observed for all the investigated equilibration processes.

Data in Figure 3 show that the cluster size distribution during the kinetics of equilibration evolves via a sequence of FS distributions. Figure 4 shows the associated time dependence of the bond probability $p(t)$, following a T -jump starting either from a high- T unbonded configuration ($p(0) = 0$) or from a previously equilibrated configuration characterized by branched

aggregates ($p(0) \neq 0$). Lines in Figure 4 are the theoretical predictions¹⁸—with the Flory post-gel assumption¹⁵ for values of $p(t)$ above percolation—i.e.

$$p(t) = p_{\text{eq}} \frac{1 - \left(\frac{1 - p(0)/p_{\text{eq}}}{1 - p(0)p_{\text{eq}}} \right) e^{-\Gamma t}}{1 - p_{\text{eq}}^2 \left(\frac{1 - p(0)/p_{\text{eq}}}{1 - p(0)p_{\text{eq}}} \right) e^{-\Gamma t}} \quad (2)$$

with $\Gamma \equiv K_{\text{site}}^{\text{breaking}}(1 + p_{\text{eq}})/(1 - p_{\text{eq}})$, where $K_{\text{site}}^{\text{breaking}}$ is the rate constant for breakage of a single bond. Since p_{eq} is known from eq 1, the entire equilibration dynamics in this aggregating branching system only depends on one parameter, $K_{\text{site}}^{\text{breaking}}$, which fixes the time scale of the aggregation process. The theoretical expression very well represents the numerical data, except for the two lowest studied temperatures ($T \leq 0.07$), at which extensively bonded states are reached ($p > 0.8$). Such disagreement can be traced to a failure of the Flory postgel assumption and/or to a progressive role of the size dependence of the cluster mobility. The overall agreement between theory and simulation in Figure 4 is further stressed by the T dependence of the single fit parameter $K_{\text{site}}^{\text{breaking}} \sim e^{-u_0/k_B T}/\sqrt{T}$ (see inset), which as expected incorporates both an Arrhenius term and the thermal velocity component $\sim \sqrt{T}$, entering the attempt rate of bond breaking.

The results of this study clearly indicate that the irreversible evolution of a system of patchy or functionalized particles, in which bonding loops can be neglected, can be put in correspondence with a sequence of equilibrium states. For this class of aggregating systems, it is thus possible to convert irreversible-aggregation time into an effective T and to envisage the evolution of a chemical gel as a progressive cooling of the corresponding physical model. Elapsed time t can be uniquely associated to an equilibrium T , recalling the concept of fictive T in aging glasses.²⁵ Equally important is the possibility of interpreting cases in which during the formation of a chemical gel the corresponding thermodynamic path crosses a thermodynamic instability line, e.g., the gas–liquid coexistence line,⁸ producing an inhomogeneous arrested structure. Such thermodynamic lines have been recently calculated with statistical mechanics methods and computer simulations.^{8,26,27} Thus, it will become possible to interpret the stability and structural properties of chemical gels by connecting them to the thermodynamic properties and to the phase diagram of the corresponding physical models.

Our study also demonstrates, for a realistic model of patchy particles, that the self-assembly kinetics of particles aggregating in loopless structures can be fully described—with no fitting parameters—by merging a thermodynamic approach providing $p_{\text{eq}}(T)$ (e.g., eq 1) with the Smoluchowski's equations studied by Van Dongen and Ernst, thus bringing reversible and irreversible aggregation of loopless branched systems to the same level of understanding as the equilibrium polymerization case.²⁰ This is made possible by the limited valence of the particles and by the specificity of the site–site interaction. The reduced valence, coupled to the nonspherical particle shape, contributes to disfavor the formation of closed bond-loops, while the specificity in the bonding interaction contributes to reduce the rate-controlling role of diffusion compared to the bonding process.¹⁹

Acknowledgment. We acknowledge support from NoE SoftComp NMP3-CT-2004-502235. We thank D. Fioretto and P. A. Rolla for helpful discussions.

References and Notes

- (1) Lehn, J.-M. *Proc. Natl. Acad. Sci. U.S.A.* **2002**, *99*, 4763.
- (2) de Greef, T. F. A.; Meijer, E. W. *Nature* **2008**, *453*, 171.
- (3) Cordier, C.-Z. P.; Leibler, L. *Nature* **2008**, *451*, 977.
- (4) Rahedi, A. J.; Douglas, J. F.; Starr, F. W. *J. Chem. Phys.* **2008**, *128*, 4902.
- (5) Odriozola, G.; Leone, R.; Schmitt, A.; Callejas-Fernández, J.; Martínez-García, R.; Hidalgo-Álvarez, R. *J. Chem. Phys.* **2004**, *121*, 5468.
- (6) Manoharan, V. N.; Elsesser, M. T.; Pine, D. J. *Science* **2003**, *301*, 483.
- (7) Mirkin, C.; Letsinger, R.; Mucic, R.; Storhoff, J. *Nature* **1996**, *382*, 607.
- (8) Bianchi, E.; Tartaglia, P.; La Nave, E.; Sciortino, F. *J. Phys. Chem. B* **2007**, *111*, 11765.
- (9) van Blaaderen, A. News and Views. *Nature* **2006**, *439*, 545.
- (10) Glotzer, S. C.; Solomon, M. J. *Nat. Mat.* **2007**,
- (11) Rubinstein, M.; Colby, R. H. *Polymer Physics*; Oxford University Press Inc.: New York, 2003.
- (12) Escobedo, F. A.; de Pablo, J. J. *J. Chem. Phys.* **1999**, *110*, 1290.
- (13) Kumar, S. K.; Douglas, J. F. *Phys. Rev. Lett.* **2001**, *87*, 188301.
- (14) Stockmayer, W. J. *J. Chem. Phys.* **1943**, *11*, 45.
- (15) Flory, P. J. *Principles of polymer chemistry*; Cornell University Press: Ithaca and London, 1953.
- (16) Martin, J.; Adolf, D. *Annu. Rev. Phys. Chem.* **1991**, *42*, 311.
- (17) Zaccarelli, E. *J. Phys.: Condens. Matter* **2007**, *19*, 323101.
- (18) van Dongen, P.; Ernst, M. J. *Stat. Phys.* **1984**, *37*, 301.
- (19) Oshanin, G.; Moreau, M. *J. Chem. Phys.* **1995**, *102*, 2977.
- (20) Cates, M. E.; Candau, S. J. *J. Phys.: Condens. Matter* **1990**, *2*, 6869.
- (21) Corezzi, S.; De Michele, C.; Zaccarelli, E.; Fioretto, D.; Sciortino, F. *Soft Matter* **2008**, *4*, 1173.
- (22) Corezzi, S.; Fioretto, D.; Rolla, P. *Nature* **2002**, *420*, 653.
- (23) De Michele, C.; Gabrielli, S.; Tartaglia, P.; Sciortino, F. *J. Phys. Chem. B* **2006**, *110*, 8064.
- (24) Wertheim, M. J. *Stat. Phys.* **1984**, *35*, 19.
- (25) Davies, R. O.; Jones, G. O. *Adv. Phys.* **1953**, *2*, 370.
- (26) Bianchi, E.; Largo, J.; Tartaglia, P.; Zaccarelli, E.; Sciortino, F. *Phys. Rev. Lett.* **2006**, *97*, 168301.
- (27) Zaccarelli, E.; Buldyrev, S. V.; Nave, E. L.; Moreno, Saika-Voivod, A. J.; Sciortino, F.; Tartaglia, P. *Phys. Rev. Lett.* **2005**, *94*, 218301.

JP809031D